Active Balancing System based on Multiple Flyback Converters for Serially Connected Lithium Battery

Chatchai Rojanasuwan[†] and **Warit Wichakool**, Non-members

ABSTRACT

This paper proposes the multiple switches-multiple flyback converters (MSMF) with an optimal algorithm of simultaneous equalization of two selected battery cells for equalizing unbalanced voltage of individual cell connected in series. Experimental results show that the proposed system achieves to equalize 24V/25Ah of a battery pack consisted of eight battery cells until the individual cell voltage has the final different value with each other less than 10mV. Each flyback converter can extract the maximum current from an individual cell approximately 8A. The MSMF reduces the balancing time by almost 45% compared to a single cell equalization algorithm.

Keywords: Active Balancing System, Lithium Battery, Battery Equalization, Flyback Converter

1. INTRODUCTION

Lithium-ion batteries are widely used in the various applications such as electric vehicles, hybrid vehicles, and the energy storage systems [1]. The interesting advantages of lithium batteries when comparing with the lead-acid batteries, which are the light weight, high energy density, low self-discharge rate, large discharge current, fast charge rate, and long lifetime [2]. However, the electrochemical characteristic of each lithium battery cell causes the cell voltage be rather small, such as a nominal voltage of lithium cobalt oxide battery (LCO) is 3.6 V, a nominal voltage of lithium manganese oxide battery (LMO) is 3 V, a nominal voltage of lithium nickel manganese cobalt battery (NMC) is 3.7 V, and a nominal voltage of lithium iron phosphate battery (LFP) is 3.2 V. Therefore, the individual cell is required to connect in series for the higher voltage of practical applications. Although, the individual cell is established from the identical type of materials, but the slight variation in the manufacturing process leads each battery cell exhibited mismatch in the internal impedance, self-discharge rate, capacity, and the temperature characteristic [3-4]. When a battery pack is charged or discharged, result to be inconsistent energy in the individual cell. Eventually, the repeated charging and discharging cycles will be rapidly increased. This situation will accelerate the deterioration of a battery pack and also reduces the available capacity [3],[5].

To mitigate the impacts of unbalanced energy in the individual cells when charging or discharging, two main methods are employed to equalize the voltage or state-of-charge (SOC) among the battery cells for reaching to the balancing voltage target. First, a passive balancing system is an equalization topology that transfers the excess energy of each cell to the dissipated energy components such as the power transistor and power resister, until the highest voltage cell decreases virtually to the lowest voltage cell. There are basically two types of a passive balancing system namely, the fixed shunting resistor and switched shunting resistor. Passive balancing system has the widespread usages due to its simplicity, reliability, and less cost characteristics. However, the concerned limitations of a passive balancing system are the thermal effect from the energy dissipation of the resistors [7-11].

Secondly, an active balancing system is considered for correcting with both the inconsistent energy of individual cell and the energy dissipation wasted in the in a passive balancing system [7-9]. By employing the ideally lossless energy components such as capacitor, inductor, transformer and converter as a tank for storing the excess energy, which is extracted from the maximum SOC cell, then transferring to the minimum SOC cell until the individual cell voltage is reached to the threshold of a balancing voltage. This method causes the excess energy to be little loss as heat when comparing with the passive balancing method, and also appropriate for the large number of serially connected battery cells [1-5]. Active balancing system can be divided into 5 types, namely, Cell bypass, Cell-to-Cell, Cell-to-Pack, Pack-to-Cell, and Cell-to-Pack-to-Cell [8]. The Cell bypass method in a paper [4] implemented n amount of the isolated dual active bridge (DAB) converters for n battery cells connected in series, Input of each DAB was parallel connected to a battery cell, Output of each DAB was mutually parallel connected to achieving the battery equalization by bypass the excess energy to the auxiliary loads. The Cell-to-Cell method in papers [12-14] applied the multi-winding transformer to transferred the energy

Manuscript received on May 16, 2024; revised on December 1, 2024; accepted on January 2, 2025. This paper was recommended by Associate Editor Chainarin Ekkaravarodome.

The authors are with Electrical Engineering and Biomedical Engineering Department at Prince of Songkla University, Hatyai Campus, Songkhla, Thailand.

[†]Corresponding author: chatchairoj40@gmail.com

Digital Object Identifier: 10.37936/ecti-eec.2525232.254126

from the highest voltage cell to the lowest voltage cell by the flyback operation and forward operation. The structure of a multi-winding transformer technique had n amounts of the winding wires connected directly to n battery cells. The restrictions of this method were the shared magnetic flux needed to reset by another circuit, and the transformer size may be large when the battery cells were serially connected in an arbitrary number [3]. In paper [15], the Cell-to-Cell method is implemented based on the switch-matrix single capacitor (SMSC) included one extra current sensor and a pairing algorithm for improving the classical structure of switch capacitor (SC), which had the fundamental disadvantages such as the energy distribution strategy that can only transferred between adjacent cells and low balancing speed when the different voltage among the cells was small. However, if the capacity of each cell is large, SMSC and SC techniques may be unsuitable due to their equalization speed are rather slow [3],[16]. The Cell-to-Pack method, the excess energy are extracted from the highest SOC cell, then transferred to a battery pack with little waste energy. Pack-to-Cell method is similar to Cell-to-Pack method, just different at the transferable energy direction between a battery pack and cells [8]. Cell-to-Pack method in paper [16] applied a buck-boost converter to achieve two stages equalization circuit. In the first stage: the energy was exchanged between cells and pack, and the second stage: the energy was exchanged between one pack and another adjacent pack, this procedure was simultaneously operated for enhancing the balancing time.

However, the limitation of a buck-boost converter is the individual cell is not isolated from a battery string. If some components in a topology are deteriorated, a battery string may be short circuit risk. Paper [6] presented the battery charge equalization and the monitoring system of battery stacks by employing a flyback converter with an auxiliary power supply to distribute the energy through a switch array and flyback converters. And also similar to papers [17-18], but the auxiliary power supply was replaced by the flyback converter, which its structure has the duplicate flyback converter performs as the central energy exchanging for charging and discharging the undercharged cell and overcharged cell, respectively. Papers [19],[20] presented Pack-to-Cell and Cell-to-Pack-to-Cell methods, which the excess energy was centrally exchanged through the single converter and the switch array. However, only one cell will be extracted the excess energy in each stage of equalization, which affect to the balancing speed when the capacities of the individual cell is large. The Cell-to-Pack method by employing a single flyback converter and the switch array to exchange the excess energy among the multiple cells and a battery string at a time, which is an advantage of this implementation [21]. However, the complexity of controlled switches that proceeds as the shared time equalization is the main limitation.

To shorten the balancing time, the multiple switches-multiple flyback converters (MSMF) with simultaneous equalization algorithm of two cells are proposed in this paper. The relay modules are employed to perform as multiple switches for eliminating amounts of converters.

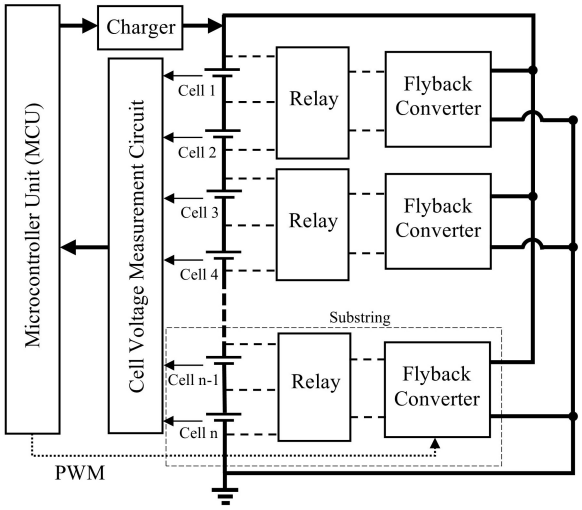

***Fig. 1**: Proposed structure of multiple switches-multiple flyback converters.*

The rest of this paper is organized as follows. The topology configuration and the fundamental operation are described in section 2. The MSMF design is presented in section 3. The experimental results of the MSMF with 25Ah lithium battery is presented in section 4. Finally, section 5 concludes this paper.

2. PROPOSED STRUCTURE

2.1 System Topology

The topology of proposed multiple switches-multiple flyback converters (MSMF) is shown in Fig. 1, which can be divided in three main circuits such as the cell measurement circuit, the microcontroller unit (MCU), and the MSMF. The system topology consists of *n* battery cells, *2n* relay modules, and *n/2* flyback converters.

A battery pack can be divided in *n/2* substrings, which each substring includes two adjacent cells connected with four relay modules and one flyback converter. The relay modules of each substring will select one maximum SOC cell for transferring the excess energy through the flyback converter. Output of all flyback converters are parallelly connected to a battery pack.

The MCU is the central processor of the proposed system for obtaining and comparing each cell voltage from the measurement circuit. Additionally, it generates the signals to control the relay modules and the multiple flyback converters for equalizing two battery cells in each equalization stage. In addition, the MCU also acts as a battery management system (BMS) in terms of protection during charging and balancing. If the MCU detects the undervoltage cell, the MCU can terminate the balancing or charging process immediately.

The auxiliary charger is employed to charges a battery

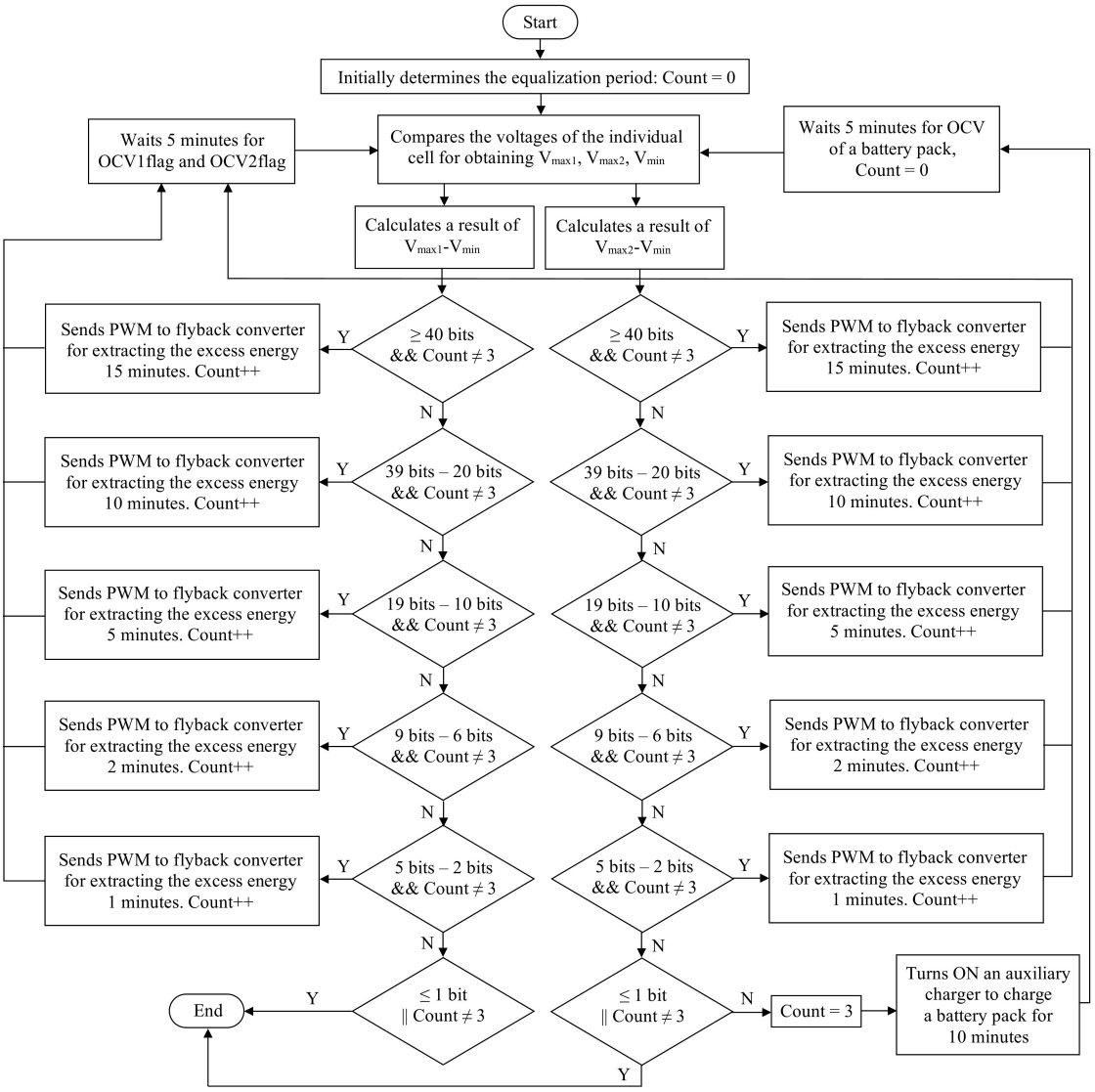

***Fig. 2**: Flowchart depicts the fundamental operation of the proposed structure.*

pack after three equalization stages are accomplished. Result to a battery pack is quickly charged due to each cell has the nearby voltage.

2.2 Fundamental Operation

In order to verify the unbalanced energy in each cell, the voltage measurement circuit is employed to measure the open circuit voltage (OCV), which the value varies directly to the SOC as an OCV-SOC curve [22].

The fundamental operation of the proposed system is shown in Fig. 2. The MCU reads voltages from a mea-surement circuit via an internal 10-bit ADC, then searches for the highest OCV of two substrings and the lowest OCV. After that, the MCU calculates different values of the first highest OCV with lowest OCV, and the second highest OCV with lowest OCV. In order to shorten the balancing time of an equalization procedure, the different values will be classified in six conditions, then the pulse width modu-lation (PWM) signals are sent to two flyback converters for extracting the excess energy according to the durations of equalized time that have been chosen.

Before the excess energy is extracted from two highest OCV cells, the multiple switches have been turned on for connecting between two selected cells and two flyback converters as shown in Fig. 3. The MCU must not employ the multiple switches to select two adjacent cells in the same substring. For example, if cell 1 is the first highest OCV cell, cell 2 is the second highest OCV cell, and cell 4 is the third highest OCV cell, according to the above mention of the flowchart in Fig. 2 cell 1 and cell 4 are selected for the simultaneous equalization of two cells.

The energy transfer procedure of entire flyback converters is defined to execute in discontinuous current mode (DCM). This procedure, the electrical energy of the highest OCV cell is converted to the magnetic energy stored in the magnetizing inductor of primary side of transformer when the MOSFET has been turned on.

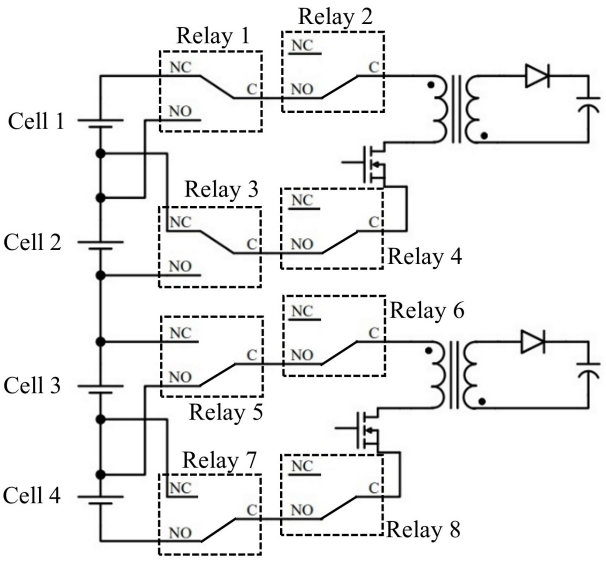

***Fig. 3**: Schematic of eight switches-two flyback converters for 4 cells connected in series.*

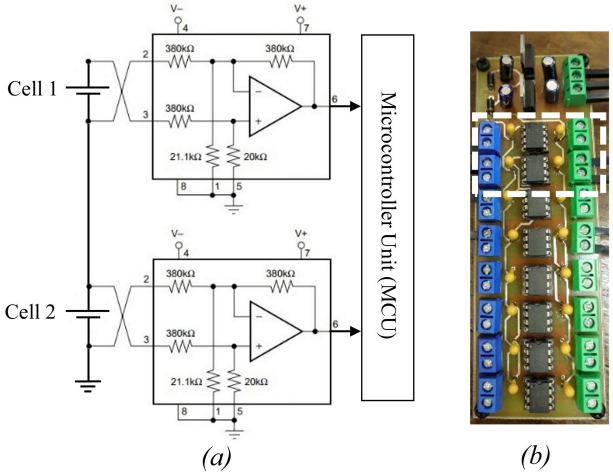

***Fig. 4**: Cell voltage measurement circuit (a) schematic diagram (b) PCB design.*

After that, the magnetic energy is transferred to the secondary side of a transformer when the MOSFET has been turned off, then the diode has operated in a forward bias mode, result in the magnetic energy is converted to the electrical energy and be distributed to a battery pack until the energy decreases linearly to zero before the next switching period is begun. In the DCM mode, the magnetic flux in a transformer will be reset. Therefore, this procedure ensures that a transfor-mer core is not saturated.

After each energy extraction has been completed, the MCU waits 5 minutes for the OCV of each cell to be stabilized. The five minutes value can be obtained by measuring the time response of 25Ah lithium battery cell after instantaneously finished discharging. An equalization period consists of three balancing stages and one charging stage. This technique will operate repeatedly until the individual cell voltage has the different values with each other less than 10 mV.

3. DESIGN CONSIDERATION

3.1 Cell Voltage Measurement Circuit

The difference amplifier is used to measure the cell voltages. The non-inverting input pin ($V_(in+)$) of the difference amplifier is connected to the positive polarity of a battery cell and the inverting input pin ($V_(in-)$) is connected to the negative polarity of a battery cell. The output pin of the difference amplifier is connected to the analog input of the MCU. The relationship between input and output of the difference amplifier can be described as

$$V_{out} = \frac{R_1}{R_2}\left(V_{in+} - V_{in-}\right). \tag{1}$$

Due to the voltage of individual cell is not higher than 5 V of a supply voltage rated of the MCU. Therefore, the unity gain of the difference amplifier is considered, specifically $R_1 = R_2$.

In order to accomplish a voltage measurement circuit, the INA117 IC is employed as shown in Fig. 4(a). The INA117 IC is the precise unity gain difference amplifier with consisting of the integrated thin film resistor network. The unity gain error of the INA117 is not more than 0.02%. PCB design of a cell voltage measurement circuit for eight battery cells has been shown in Fig. 4(b).

3.2 Flyback Converter

According to the above mentioned, the flyback converter requires the DCM operation as shown in Fig. 5. The magnetizing inductor current increases linearly with the time duration when the switch is turned on. After that the magnetizing inductor current decreases linearly to zero when the switch is turned off. Hence, the transformer design of a flyback converter can be described as

$$I_{avg} = \frac{1}{T}\int_0^T i(t)dt, \tag{2}$$

$$I_{cell,avg} = \frac{1}{2}\left(i_{cell,max}\right)(DT)\left(\frac{1}{T}\right), \tag{3}$$

$$I_{cell,avg} = \frac{1}{2}Di_{cell,max}. \tag{4}$$

The relationship between voltage and current of the magnetizing inductor in a transformer when the switch is turned on, which can be described as

$$v_{cell} = L_m\frac{di_{L_m}}{dt}, \tag{5}$$

$$L_m = \frac{V_{cell}DT}{i_{cell,max}}, \tag{6}$$

where $i_{cell,max}$ is a maximum cell current that be extracted to a transformer. $I_{cell,avg}$ is an average current that can be evaluated by an area under the triangular

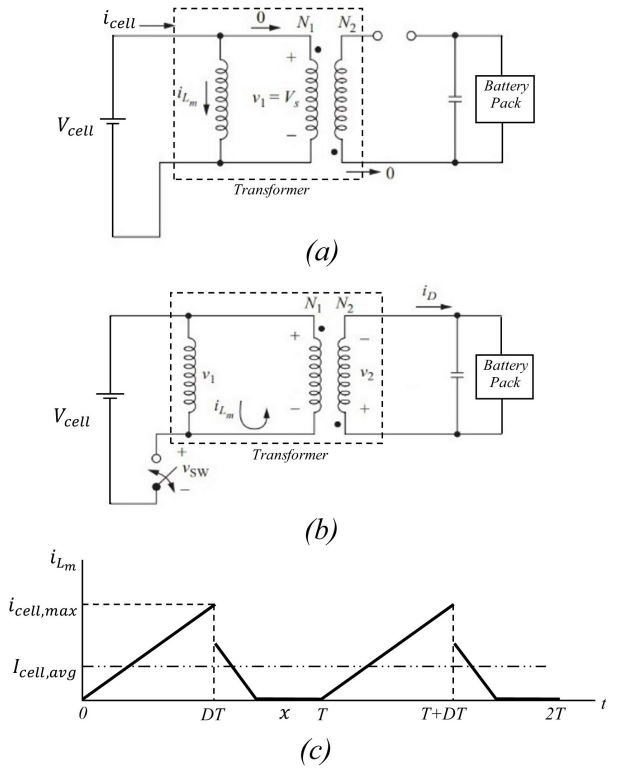

***Fig. 5**: : Operations of a flyback converter (a) switch is turned on (b) switch is turned off (c) discontinuous current mode.*

waveform in a switching period. L_m is a magnetizing inductance. D is a duty cycle and T is a switching period.

We define the suitable value of the average current approximately 2.5A, limiting the trans-former size and also extracts high current from cells. The switching frequency is defined to be 100kHz, which is an appropriate value for achieving the compact size of com-ponents in a flyback converter such as a transformer core is small, a capacitor size at the output of flyback converter will be reduced. A duty cycle is defined to be 0.5, which is suitable value for achieving the DCM state in the flyback converter.

Therefore, we can evaluate $i_{cell,max}$ from equation (4), that equals to 10A. V_{cell} is a battery cell voltage, that has the value among 2.7V to 3.4V. From equation (6), we can evaluate the magnetizing inductance of a transformer, that equals to 1.35μH. Amount of the primary winding turns, turn ratio between the primary winding and the secondary winding of a transformer can be described as

$$N_p = \frac{DV_{cell,\max}}{A_c B_m f_{sw}}, \tag{7}$$

$$n = \frac{N_s}{N_p} = \left(\frac{V_{pack} + V_{diode}}{V_{cell,\min}}\right)\left(\frac{1 - D - x}{D}\right), \tag{8}$$

where A_c is core area of a transformer. B_m is the magnetic flux density, which its value is 200mT. V_{pack} is a battery pack voltage, that has the defined voltage as 26V, V_{diode} is a forward voltage across a diode and x is a

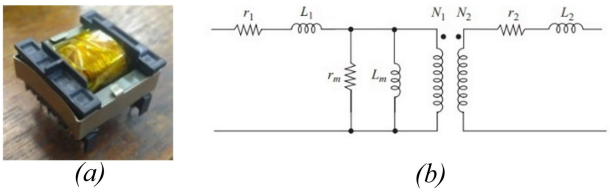

***Fig. 6**: Transformer of a flyback converter (a) established prototype (b) equivalent circuit.*

constant value defined to maintain the DCM operation in a transformer, which the defining value is approximated to 0.02 because the highest voltage cell is required to extract the excess energy as more as possible for attaining the less balancing time. If we substitute the values into equation (7) and (8), we will get the values of $n = 10$, $N_p = 3$, and $N_s = 30$. The gap length of transformer core can be described as

$$l_g = \frac{\mu_0 A_c N_p^2}{L_m}, \tag{9}$$

$$A_p = A_c \times A_w, \tag{10}$$

$$A_p = \frac{P_{out}\left(\frac{1}{\eta}\sqrt{\frac{4D}{3}} + \sqrt{\frac{4(1-D)}{3}}\right)}{J K_w B_m f_{sw}}, \tag{11}$$

where μ_0 is the permeability of free space. The selection of a transformer core is estimated by the area product strategy described as equation (10) and (11), where P_{out} is the output power of transformer, η is an efficiency defined to 0.85, J is a current density defined to 5 A/mm2, and K_w is the window utilization factor defined to 0.4.

First, we calculate the area product in equation (11), then compare to the multiplying value of the core area and winding area of a selected transformer core from equation (10). The comparison result of a selected core must be higher than a calculated value. Hence, the TDK B66311 ferrite core with 0.25mm of gap length was selected for the implementation.

A transformer of flyback converter operated in DCM has been established as shown in Fig. 6(a). The parameters of established transformer have presented in Fig. 6(b). Transformer parameters were measured and shown in Table 1.

MATLAB simulation results using measured parameters are shown in Fig. 7. The spike voltages and the oscillated voltages occurred at the onset of turning-off the MOSFET, which were caused by the leakage inductance of a transformer and the parasitic capacitance of the MOSFET, which could result in the breakdown of the MOSFET.

To fix these problems, the RCD clamp circuit and the RC snubber circuit employed as shown in Fig. 9(a). The RCD clamp circuit is coupled connectedly to a transformer for reducing the spike voltage. The RC snubber circuit is coupled connectedly to the MOSFET for

***Table 1**: The measured parameters of transformer.*

Magnetizing inductance (L_m)	1.47 µH
Primary leakage inductance ($L_{1,leak}$)	0.44 µH
Primary internal resistance (r_1)	0.11 Ω
Magnetizing resistance (r_m)	10,000 Ω
Secondary inductance (L_s)	110 µH
Secondary leakage inductance ($L_{2,leak}$)	52 µH
Secondary internal resistance (r_2)	1.3 Ω
Turn ratio (N_s/N_p ; n)	8.65
Switching frequency (f_{sw})	100 kHz

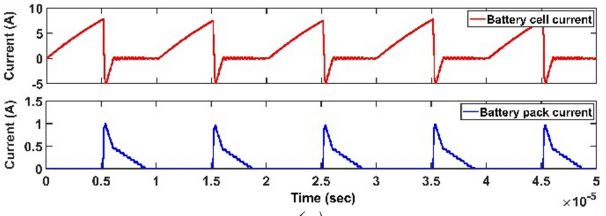

(a)

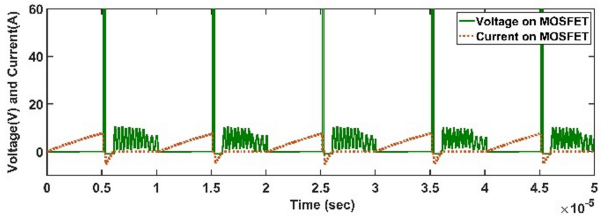

(b)

***Fig. 7**: Simulation results of a flyback converter without RCD clamp and RC snubber circuits (a) current variation in a transformer (b) V_{ds} and I_{ds} were occurred at the MOSFET.*

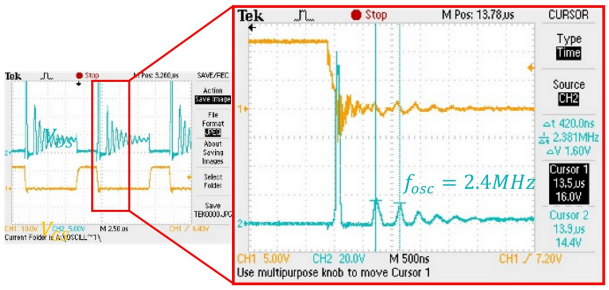

***Fig. 8**: Oscillated voltage was occurred at the MOSFET.*

***Table 2**: Component values of RCD and RC circuits .*

RCD clamp circuit		RC snubber circuit	
R_{clamp}	*80 Ω*	$R_{snubber}$	*10 Ω*
C_{clamp}	*0.47 µF*	$C_{snubber}$	*10 nF*
Diode	*MCCUS5B*		

mitigating the oscillated voltage occurred across drain-source pin.

Components of RCD clamp circuit can be calculated by

$$R_{clamp} = \frac{2V_{clamp}\left(V_{clamp} - \frac{V_{pack,flyback}}{n}\right)}{f_{sw}L_{1,leak}I^2_{cell,\max}}, \quad (12)$$

$$V_{clamp} = V_{peak} - V_{cell}, \quad (13)$$

$$C_{clamp} = \frac{5}{f_{sw}R_{clamp}}. \quad (14)$$

Components of RC snubber circuit can be calculated by

$$C_{parasitic} = \frac{1}{\left(2\pi f_{osc}\right)^2 L_{1,leak}}, \quad (15)$$

$$R_{snubber} = \sqrt{\frac{L_{1,leak}}{C_{parasitic}}}, \quad (16)$$

$$C_{snubber} = \frac{P_{loss}}{V^2_{ds}f_{sw}}, \quad (17)$$

where V_{peak} is the target peak of spike voltage, which is defined as 15 V. $V_{pack,flyback}$ is a battery pack voltage reflected to the primary winding of a transformer, and n is a turn ratio of a transformer. $C_{parasitic}$ can be estimated from equation (15). f_{osc} can be obtained by measuring the oscillated frequency occurred at the V_{ds} pin of MOSFET as shown in Fig. 8. P_{loss} is power loss in the snubber circuit, which is defined as 50 mW. Therefore, we can estimate the component values in the RCD clamp circuit and RC snubber circuit, which are shown in Table 2.

Simulation results of the flyback converter with RCD clamp and RC snubber circuits are shown in Fig. 9. The spike voltage occurred at the MOSFET is decreased to 20 V. Likewise with the oscillated voltage occurred at the MOSFET is also reduced by the RC snubber circuit.

An appropriate duty cycle of the PWM signal was investigated, due to the measured parameters of the actual transformer from Table 1 have an impact to the original determination of PWM duty cycle, which equals to 0.5. Therefore, we need to simulate the flyback converter from Fig. 9(a) again, by determining 50%, 60%, and 70% of duty cycle values. The duplicate simulation results of a flyback converter are shown in Fig. 10. Simulation results in Fig. 10, the maximum boundary of duty cycle for DCM operation should be 60%, which enable the transformer core to be completely reset.

PCB design of a flyback converter is shown in Fig. 11, which consist of two independent and identical design of flyback converters. PC923L IC with isolated supply were used to drive the gate of the MOSFET, which achieve the ground isolation between MCU and flyback converter.

3.3 Microcontroller Unit

Arduino mega2560 is employed as the MCU of the proposed system. It can achieve the digital values of each cell via 10-bit resolution of analog to digital conversion

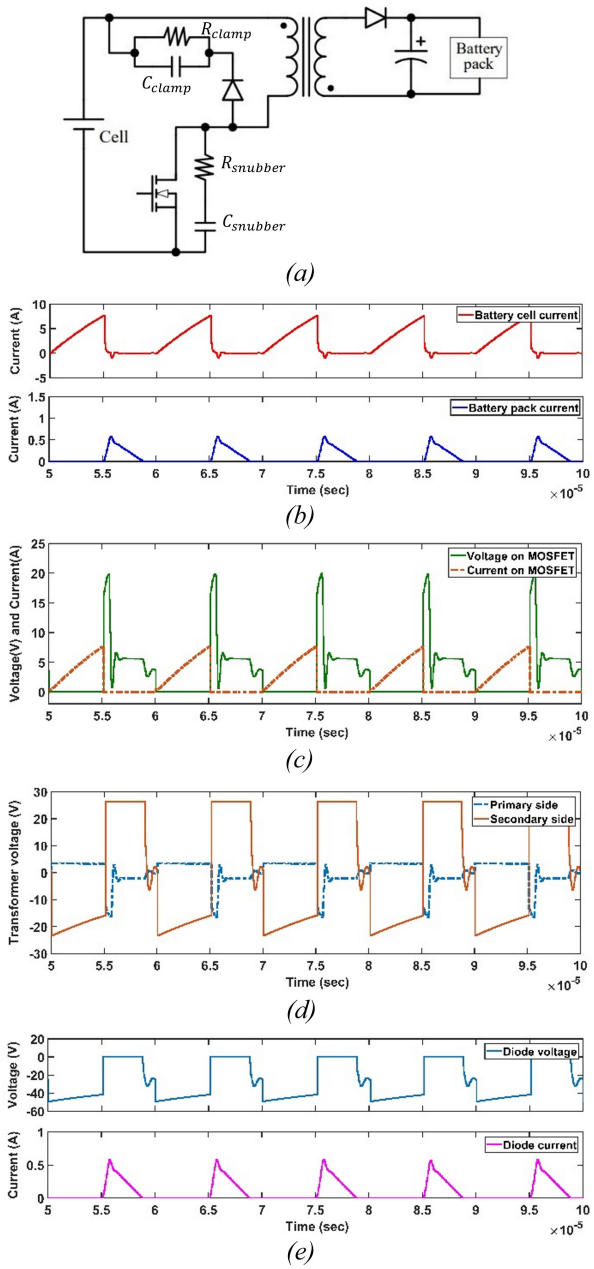

***Fig. 9**: Simulation results of a flyback converter (a) RCD clamp and RC snubber circuits were implemented (b) current variation in a transformer (c) V_{ds} and I_{ds} were occurred at the MOSFET (d) voltage variation in a transformer (e) voltage and current of a diode.*

(ADC). Table 4 presents the digital values of each cell, which have been converted by the equation (18) and (19)

$$Resolution = \frac{5}{2^{10}} = 4.88\,\text{mV}, \tag{18}$$

$$Digital\ value = \frac{V_{cell} \times 1024}{5}. \tag{19}$$

The balancing voltage of the proposed system can be determined by the different results of digital values among each battery cell, which the results must less than

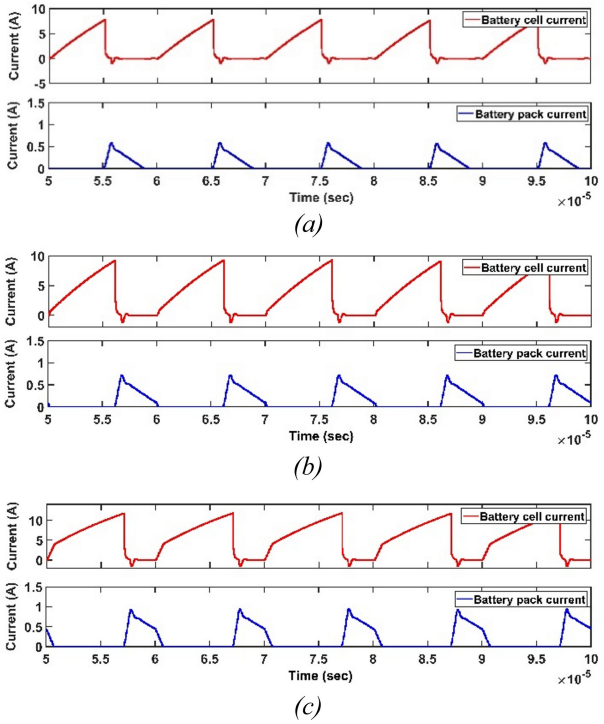

***Fig. 10**: Simulation results of a flyback converter for determining the appropriate duty cycle of PWM signal (a) duty cycle 50% (b) duty cycle 60% (c) duty cycle 70%.*

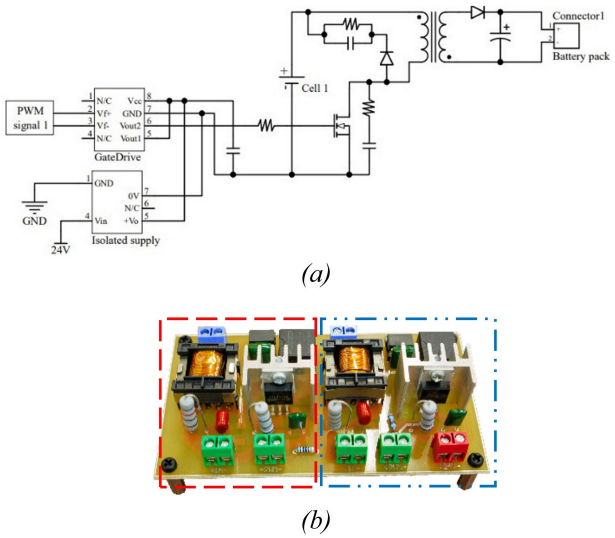

***Fig. 11**: Two independent and identical design of flyback converters (a) schematic diagram (b) PCB design.*

or equal to 1. In other words, the balancing voltage difference after balancing should be less than 9.76 mV.

The ADC of Arduino mega2560 is enabled by writing logical one or zero into the ADCSRA, ADCSRB, and ADMUX registers. Timer0, 1, 2, 5 are used for interrupting the events when each timer matches the TOP value. The interrupted frequency can be calculated by

$$f_{OCnA} = \frac{f_{clock}}{N(1 + OCRnA)}, \tag{20}$$

***Table 3**: Component values of a flyback converter.*

Transformer	*TDK B66311*
MOSFET	*IRLB8748PBF*
Diode	*MCCUS5B*
Output Capacitor	*47μF 50V*
Gate Driver	*PC923L*
Isolated Supply	*WRB2412ST*

***Table 4**: Digital values of individual cell voltage.*

Individual cell voltage	Digital value
0 mV – 4.88 mV	*0*
4.88 mV – 9.76 mV	*1*
9.76 mV – 14.64 mV	*2*
14.64 mV – 19.52 mV	*3*
19.52 mV – 24.4 mV	*4*
⋮	
4.982 V – 4.987 V	*1021*
4.987 V – 4.992 V	*1022*
4.992 V – 4.997 V	*1023*

***Table 5**: Voltage measurement results.*

Voltages measured by Siglent SDM 3055		Voltages measured by difference amplifier		% Error
Cell 1	*3.2884 V*	*Cell 1*	*3.2913 V*	*0.09*
Cell 2	*3.2836 V*	*Cell 2*	*3.2855 V*	*0.06*
Cell 3	*3.2837 V*	*Cell 3*	*3.2845 V*	*0.02*
Cell 4	*3.2722 V*	*Cell 4*	*3.2729 V*	*0.02*
Cell 5	*3.2860 V*	*Cell 5*	*3.2862 V*	*0.01*
Cell 6	*3.2717 V*	*Cell 6*	*3.2718 V*	*0.01*
Cell 7	*3.2807 V*	*Cell 7*	*3.2789 V*	*0.05*
Cell 8	*3.2775 V*	*Cell 8*	*3.2763 V*	*0.04*

where N is the prescaler divider such as 1, 8, 64, 256, or 1024 and n is the timer/counter number. The interrupt can be enabled by writing logical one or zero in the TCCRnA, TCCRnB, TCNTn, OCRnA, OCRnB, OCRnC, TIFRn, and TIMSKn registers.

Timer3 and 4 are used for generating PWM signals, which their frequencies can be calculated by

$$f_{OC3A,PWM} = \frac{f_{clock}}{N(1 + OCRnA)}, \tag{21}$$

where OCRnA is a register indicated the switch frequency of flyback converter.

For the duty cycle calculation of PWM signal, The OCRnB and OCRnC registers can be calculated by

$$1 + OCRnB = f_{clock} \times DT_{switching}. \tag{22}$$

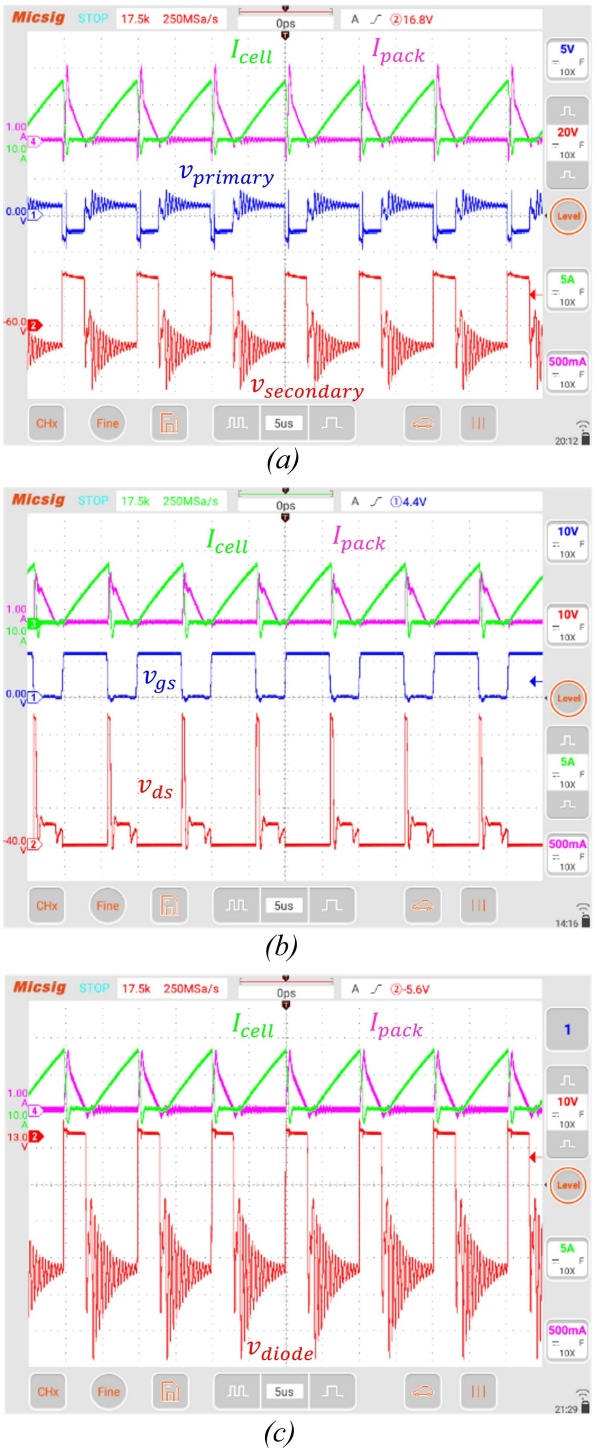

***Fig. 12**: Operation waveform of a flyback converter (a) current and voltage variations in a transformer (b) current and voltage variations at the MOSFET (c) current and voltage variations at a diode.*

4. EXPERIMENTAL RESULTS

4.1 Cell Voltage Measurement Results

Table 5 shows the output voltages of the difference amplifier and cell terminal voltages measured by the 5.5 digits digital multimeter of Siglent SDM 3055, which the

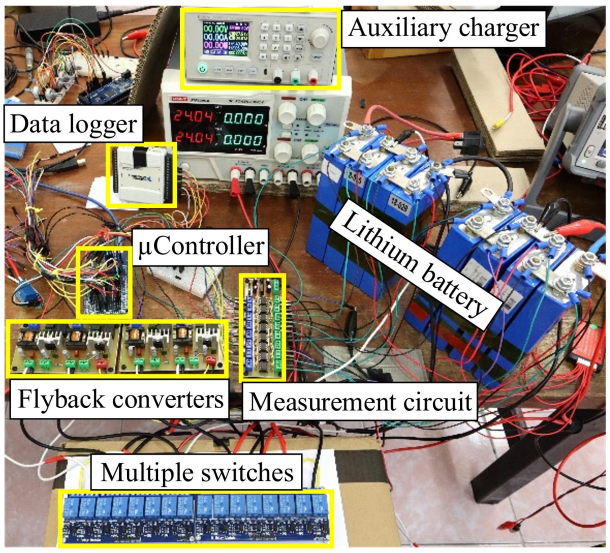

***Fig. 13**: Experiments of the MSMF with 24V battery pack .*

comparison results show that the difference amplifier and 10-bit ADC combination is accurate enough for the purposed cell voltage balancing.

4.2 Flyback Converter Operations

PCB prototype of flyback converter in Fig. 11(b) was tested with a battery pack consisted of eight cells serially connected. Input of flyback converter was connected with relay modules to select cell from each substring and output was connected to a battery pack terminal. PWM signals with a duty cycle 60% of switching period were distributed to drive the MOSFETs.

The operation results of a flyback converter are shown in Fig. 12. From the results, the flyback converter can operate in the DCM. RCD clamp and RC snubber circuits can reduce the spike voltages and oscillated voltages on the drain-source pin of MOSFET as shown in Fig. 12(b)

4.3 Cell Equalization Results

Experiments of the MSMF were demonstrated with 24V battery pack consisted of eight lithium battery cells connected in series is shown in Fig. 13. The capacity of each cell was approximately 25Ah. Four experiments are shown in this paper. First, the MSMF with a single cell equalization algorithm was tested. Second, the MSMF with optimal algorithm of two cells balancing was tested to compare to the first experiment. In the third and fourth experiments, the MSMF with optimal algorithm of two cells balancing was tested to equalize with different initial cell voltages.

In the first experiment, an initial voltage of cell 4 was close to 3.08 V and other cells were close to 3.18 V. The different voltage between cell 4 and other cells was close to 0.1 V as shown in Fig. 14(a). Experimental result shows that the MSMF with algorithm of single cell balancing can equalize the inconsistent voltages of each cell until

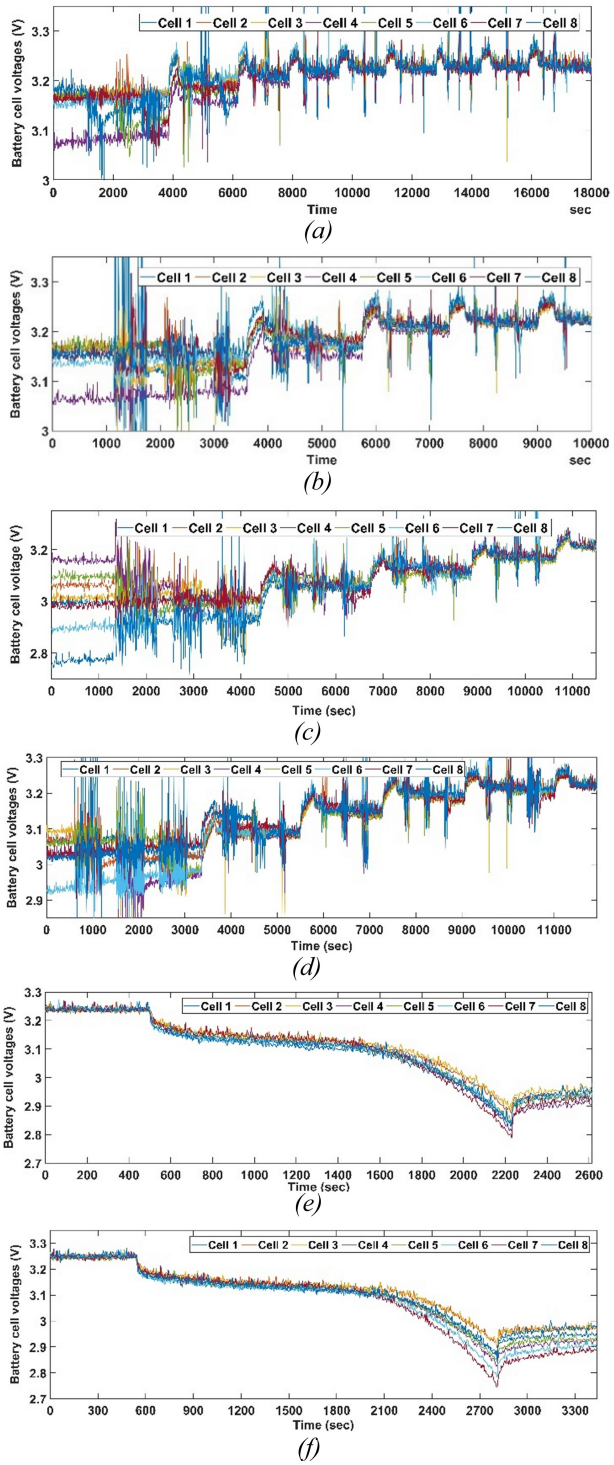

***Fig. 14**: Experimental results of the MSMF with 24V battery pack (a) first experiment (b) second experiment (c) third experiment (d) fourth experiment (e) discharging result of 150W constant power case (f) discharging result of 6A constant current case.*

the cell voltage difference is less than 10 mV with the duration time of 18,000 seconds or 5 hours.

In the second experiment, an initial voltage of cell 4 was close to 3.06V and other cells were close to 3.16V.

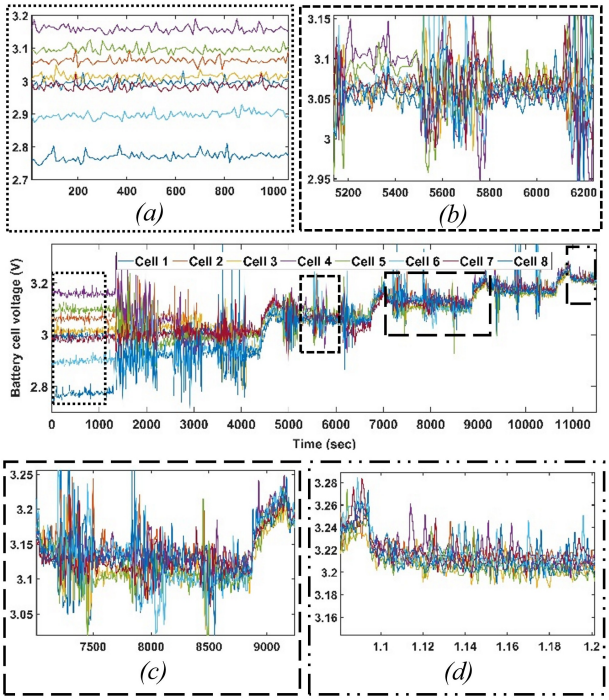

***Fig. 15**: Voltage waveforms of individual battery cell in the third experiment (a) before the MSMF was implemented (b) two cells equalization strategy was operated (c) equalization period consisted of three equalized stages and one charging stage (d) after the MSMF was stopped.*

The different voltage between cell 4 and other cells was close to 0.1V as shown in Fig. 14(b) and Fig. 16(a). Experimental result shows that the MSMF with optimal algorithm of two cells balancing time is reduced to 10,000 seconds or 2.7 hours. Comparing to the first experiment, the balancing time can be reduced by almost 45%.

In the third experiment, an initial voltage of each cell was set to be the worst case, which individual cell had the various voltage as shown in Fig. 14(c) and Fig. 16(b). The MSMF with an optimal algorithm was demonstrated. Experimental result shows that the unbalanced voltage of each cell can be close to the balancing voltage with 11,050 seconds or 3 hours.

In the fourth experiment, an initial voltage difference between the highest and lowest cell was approximate to 0.17V as shown in Fig. 14(d) and Fig. 16(c). Unbalanced energy of individual cell was equalized with the proposed MSMF. The balancing time until the final different voltage of each cell was less than 10mV were 11470 seconds or approximately 3 hours as shown in Fig. 16(c) at the orange bar charts.

Fig. 14(e) and Fig. 14(f) show the discharging result of 150W constant power case and 6A constant current case after the MSMF has been employed. In the first duration of discharging, the individual cell voltage was gradually decreased with the nearby value. Until the final duration of discharging, the individual cell voltage rapidly decreased, result to each cell was inconsistent voltage.

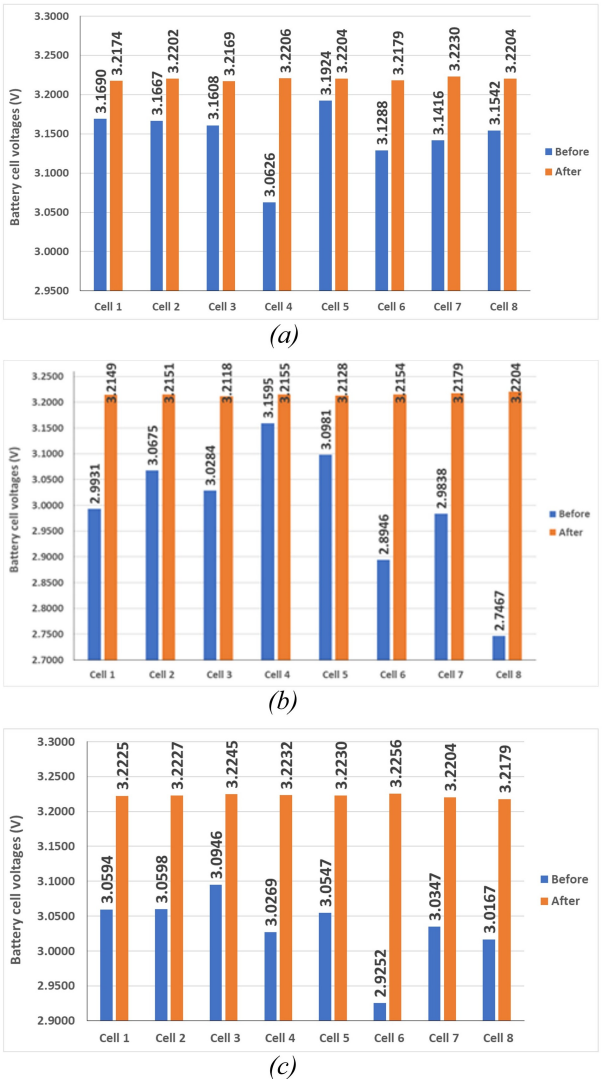

***Fig. 16**: Bar chart shows the individual cell voltage before and after implementing the MSMF (a) second experiment (b) third experiment (c) fourth experiment.*

Fig. 15 shows the third experiment details, which are divided in four groups. Fig. 15(a) indicated the unbalanced voltages of each cell before implementing the MSMF. Fig. 15(b) indicated an operation of the MSMF with an optimal algorithm. In each operation, the voltage spikes were occurred due to the MSMF extracting current at the high frequency switching. Result in the recorded voltages of a data logger have varied rather high values due to the setting of recorded rate is equal to 10 seconds per data. After the equalization procedure finished, the occurred spires of each cell voltage were reduced to the normal voltage. Fig. 15(c) indicated an equalization period consisted of three equalized stages and one charging stage. Finally, Fig. 15(d) indicated the balanced voltages of each cell after the MSMF operation was stopped.

In case of the battery pack is depleted or the battery cell is over discharged or undervoltage, the MCU can

terminate the balancing or the charging process because it has the individual cell voltage reading and battery pack voltage. As a result, the MCU perform a protection task of the battery management system. It can be used to notify the bad battery cell to be replaced.

The MSMF has been proposed for equalizing the inconsistent voltages in eight battery cells connected in series, which their capacity is 25Ah. The MSMF prototype has achieved the final different voltages of individual cell less than 10mV. Also shorten approximately 45% with an optimal algorithm of two cells balancing when comparing to a single cell equalization algorithm. The second reason that the proposed system can shorten the balancing time is the maximum current extraction of each flyback converter has achieved approximately 8A.

5. CONCLUSION

An active balancing system based on the multiple switches-multiple flyback converters (MSMF) with an optimal algorithm of two cells balancing is proposed for equalizing unbalanced energy in the large capacity of each battery cell connected in series. The system topology consists a relay module connected parallelly between two battery cells and one flyback converter as a substring. Output of all substrings are parallelly connected to the battery pack and auxiliary charger. The prototype of proposed system is demonstrated with 25Ah-8cells of lithium phosphate batteries. The experimental results show that the proposed system is successful for the energy equalization of inconsistent cell voltage until the final voltage difference of individual cell is less than 10mV. Also successful to shorten the balancing time with the strategy of two cells simultaneity equalization.

The proposed system can be continued to develop in term of efficiency increasing or in term of size reduction, such as choosing the PQ core or pot core for reducing the leakage magnetic flux in transformer of flyback converter, or choosing the MOSFETs for replacing instead the relay modules, respectively. Finally, we can further reduce the duration time of a balancing procedure by increasing the number of active flyback converters.

REFERENCES

[1] F. Qu, Q. Luo, H. Liang, D. Mou, P. Sun, and X. Du, "Systematic Overview of Active Battery Equalization Structures: Mathematical Modeling and Performance Evaluation," in *IEEE Transactions on Energy Conversion*, vol. 37, no. 3, pp. 1685-1703, Sep 2022.

[2] L. Tian, M. Hong, Z. He, and M. Gao, "Active Battery Balancing Circuit Based on Optimized Flyback Convertor for Large Lithium-ion Battery Packs," *IEEE 4th International Conference on Control Science and Systems Engineering (ICCSSE)*, Wuhan, China, pp. 212-216, 2018.

[3] X. Qi, Y. Wang, M. Fang, Y. Wang, and Z. Chen, "Multiport DC–DC Converter with Integrated Cascaded Structure for Optimizing Centralized Battery Equalization System," in *IEEE Transactions on Power Electronics*, vol. 37, no. 12, pp. 15111-15126, Dec 2022.

[4] M. Evzelman, M. M. U. Rehman, K. Hathaway, R. Zane, D. Costinett, and D. Maksimovic, "Active Balancing System for Electric Vehicles with Incorporated Low-Voltage Bus," *IEEE Transactions on Power Electronics*, vol. 31, no. 11, pp. 7887-7895, Nov 2016.

[5] X. Guo, J. Geng, Z. Liu, X. Xu, and W. Cao, "A Flyback Converter-Based Hybrid Balancing Method for Series-Connected Battery Pack in Electric Vehicles," *IEEE Transactions on Vehicular Technology*, vol. 70, no. 7, pp. 6626-6635, 2021.

[6] T. Conway, "An Isolated Active Balancing and Monitoring System for Lithium-ion Battery Stacks Utilizing a Single Transformer Per Cell," *IEEE Transactions on Power Electronics*, vol. 36, no. 4, pp. 3727-3734, 2021.

[7] R. Li, P. Liu, K. Li, and X. Zhang, "Research on Retired Battery Equalization System Based on Multi-Objective Adaptive Fuzzy Control Algorithm," *IEEE Access*, vol. 11, pp. 89535-89549, 2023.

[8] Z. B. Omariba, L. Zhang, and D. Sun, "Review of Battery Cell Balancing Methodologies for Optimizing Battery Pack Performance in Electric Vehicles," in *IEEE Access*, vol. 7, pp. 129335-129352, 2019.

[9] L. A. Perişoară, I. C. Guran, and D. C. Costache, "A Passive Battery Management System for Fast Balancing of Four LiFePO4 Cells," *2018 IEEE 24th International Symposium for Design and Technology in Electronic Packaging (SIITME)*, Iasi, Romania, pp. 390-393, 2018.

[10] K. Vitols, "Redesign of passive balancing battery management system to active balancing with integrated charger converter," *2014 14th Biennial Baltic Electronic Conference (BEC)*, Tallinn, Estonia, pp. 241-244, 2014.

[11] R. Paidi and S. K. Gudey, "Active and Passive Cell Balancing Techniques for Li-Ion Batteries used in EVs," *2022 IEEE International Power and Renewable Energy Conference (IPRECON)*, Kollam, India, pp. 1-6, 2022.

[12] Y. Chen, X. Liu, Y. Cui, J. Zou, and S. Yang, "A MultiWinding Transformer Cell-to-Cell Active Equalization Method for Lithium-Ion Batteries With Reduced Number of Driving Circuits," *IEEE Transactions on Power Electronics*, vol. 31, no. 7, pp. 4916-4929, 2016.

[13] S. Li, C. C. Mi, and M. Zhang, "A High-Efficiency Active Battery-Balancing Circuit Using Multiwinding Transformer," *IEEE Transactions on Industry Applications*, vol. 49, no. 1, pp. 198-207, 2013.

[14] Y. Shang, B. Xia, C. Zhang, N. Cui, J. Yang, and C. Mi, "A Modularization Method for Battery Equalizers Using Multiwinding Transformers," *IEEE Transactions on Vehicular Technology*, vol. 66, no.

10, pp. 8710-8722, 2017.

[15] P. H. La and S. J. Choi, "Direct Cell-to-Cell Equalizer for Series Battery String Using Switch-Matrix Single-Capacitor Equalizer and Optimal Pairing Algorithm," *IEEE Transactions on Power Electronics*, vol. 37, no. 7, pp. 8625-8639, 2022.

[16] X. Ding et al., "A Novel Active Equalization Topology for Series-Connected Lithium-ion Battery Packs," *IEEE Transactions on Industry Applications*, vol. 56, no. 6, pp. 6892-6903, 2020.

[17] M. A. Hannan, M. M. Hoque, S. E. Peng, and M. N. Uddin, "Lithium-Ion Battery Charge Equalization Algorithm for Electric Vehicle Applications," *IEEE Transactions on Industry Applications*, vol. 53, no. 3, pp. 2541-2549, 2017.

[18] K. Yu, Y. Shang, X. Wang, N. Wang, B. Duan, and C. Zhang, "A Multi-Cell-to-Multi-Cell Equalizer for Series-Connected Batteries Based on Flyback Conversion," *2019 3rd Conference on Vehicle Control and Intelligence (CVCI)*, Hefei, China, pp. 1-5, 2019.

[19] L. A. Perișoară, D. C. Costache, I. C. Guran, R. Ș. George, and A. Florescu, "Active Balancing for Efficient Management of a 4S1P LiFePO4 Battery Pack," *2019 11th International Symposium on Advanced Topics in Electrical Engineering (ATEE)*, Bucharest, Romania, pp. 1-6, 2019.

[20] J. Lu, Y. Wang, and X. Li, "Isolated Bidirectional DC–DC Converter with Quasi-Resonant Zero-Voltage Switching for Battery Charge Equalization," *IEEE Transactions on Power Electronics*, vol. 34, no. 5, pp. 4388-4406, 2019.

[21] A. M. Imtiaz and F. H. Khan, "Time Shared Flyback Converter Based Regenerative Cell Balancing Technique for Series Connected Li-Ion Battery Strings," *IEEE Transactions on Power Electronics*, vol. 28, no. 12, pp. 5960-5975, 2013.

[22] Y. Song, M. Park, M. Seo, and S. W. Kim, "Improved SOC estimation of lithium-ion batteries with novel SOC-OCV curve estimation method using equivalent circuit model," *2019 4th International Conference on Smart and Sustainable Technologies (SpliTech)*, Split, Croatia, pp. 1-6, 2019.

Chatchai Rojanasuwan received the B.Eng. degree in electronics from King Mongkut's Institute of Technology Ladkrabang, Bangkok, Thailand, in 2014. He is pursuing the M.Eng. degree in electrical engineering with Prince of Songkla University, Hatyai Campus, Songkhla, Thailand. His research interests power converter and applications in renewable energy.

Warit Wichakool received the Ph.D. degree in electrical engineering and computer science from the Massachusetts Institute of Technology, Cambridge, MA, USA, in 2011. He is currently working at Electrical Engineering and Biomedical Engineering Department at Prince of Songkla University, Hatyai Campus, Songkhla, Thailand. His current research interests include power system analysis, power converter and applications in renewable energy.